RSC Advances

PAPER

Cite this: *RSC Adv.*, 2016, **6**, 11023

Catalyzed Claisen–Schmidt reaction by protonated aluminate mesoporous silica nanomaterial focused on the (*E*)-chalcone synthesis as a biologically active compound

Mohammad Reza Sazegar,*[ab] Shaya Mahmoudian,[c] Ali Mahmoudi,[a] Sugeng Triwahyono,[bd] Aishah Abdul Jalil,[e] Rino R. Mukti,[f] Nur H. Nazirah Kamarudin[e] and Monir K. Ghoreishi[c]

The mesoporous silica structure (MSN) was synthesized using the sol–gel method followed by aluminum grafting and protonation and was then denoted as HAlMSN (Si/Al = 18.9). N_2 physisorption confirmed the mesoporous structure with a pore diameter of 3.38 nm. ^{27}Al NMR showed the presence of framework and extra-framework aluminum structures, which led to the formation of strong Lewis and Brønsted acidic sites. HAlMSN catalyzed the synthesis of (*E*)-chalcones through the Claisen–Schmidt reaction. Chalcone derivatives have been applied as biologically active compounds with anti-cancer, anti-inflammatory and diuretic pharmacological activities. The products were obtained *via* reactions on the protonic acid sites of HAlMSN. The significant advantages of this reaction are high yield, easy work up, short reaction time and also compatibility with various organic solvents. The products were obtained in an excellent conversion of 97% at 298 K. The results show that the electron donating substituents exhibit higher conversion in comparison to electron withdrawing substituents. The stability of the catalyst was investigated by reusing it five times for (*E*)-chalcone production and there was only a slight decrease in its catalytic activity. The highest product of (*E*)-chalcone was observed with a 1 : 2 molar ratio of benzaldehyde/acetophenone. A comparative study in chalcone synthesis using the heterogeneous catalysts demonstrated that HAlMSN has a significantly high activity at low temperature.

Received 6th November 2015
Accepted 5th January 2016

DOI: 10.1039/c5ra23435b

www.rsc.org/advances

Introduction

The hierarchically mesoporous siliceous nanostructures (MSN) with specific properties such as high internal surface areas (500–1000 $m^2\ g^{-1}$), large uniform pore dimensions (2–50 nm) and large pore volumes have received significant attention from researchers.[1] Their properties make them suitable for various applications in the different fields of science: *e.g.* drug delivery, environmental refinery, petroleum science and chemical reactions.[2] In these types of catalysts, the presence of acid sites plays a major role in their catalytic activities and since the pure MSN does not have Lewis and Brønsted acid sites in its structure, it cannot be used as a strong acid catalyst.[3] In order to improve its acid sites and subsequently modify its catalytic activity, incorporation of some metals such as aluminum,[4] nickel[1] and platinum[5] into the MSN framework has been reported. These metals are effective for creating Brønsted acid sites in the structures.[3,6,7] However, this method is limited to making Brønsted acid sites of moderate strength. The pure MCM-41 is a mesoporous silica material that is widely used in various applications as a catalyst. Introduction of aluminum into MCM-41 increases its catalytic activity due to the generation of Lewis and Brønsted acid sites in the structure,[8] which results in its being used as a solid acid catalyst.[9] In addition, some transition metals like Pt, Zr, Ni, Ir and Zn are able to improve the activity of the nanomaterials.[4,9–13] The mesoporous silica nanoparticles are capable of catalyzing the synthesis of some chemical compounds,[9] especially in the pharmaceutical industries and medicinal chemistry.[4,12] Therefore, Al-grafted MCM-41 can be used for the synthesis of (*E*)-chalcone derivatives, which have been used in the pharmaceutical science industries.[14]

[a]*Dept. of Chemistry, Fac. of Science, North Tehran Branch, Islamic Azad University, Tehran, Iran. E-mail: m_r_sazegar@yahoo.com; Tel: +98-2122262564*

[b]*Dept. of Chemistry, Fac. of Science, Universiti Teknologi Malaysia, 81310 UTM Johor Bahru, Johor, Malaysia*

[c]*Dept. of Polymer, Fac. of Engineering, Kashan Branch, Islamic Azad University, Kashan, Iran*

[d]*Ibnu Sina Institute for Fundamental Science Studies, Fac. of Science, Universiti Teknologi Malaysia, 81310 U TM Johor Bahru, Johor, Malaysia*

[e]*Institute Hydrogen Economy, Dept. of Chemical Eng., Fac. of Chemical Eng., Universiti Teknologi Malaysia, 81310 UTM Johor Bahru, Johor, Malaysia*

[f]*Division of Inorganic and Physical Chemistry, Fac. of Mathematics and Natural Sciences, Institut Teknologi Bandung, JlGanesha No 10, Bandung, 40132 Indonesia*

The (*E*)-chalcone family ((*E*)-1,3-diaryl-2-propenone) is a subgroup of the flavonoids, which has been displayed as biologically active compounds. These materials could act as anti-cancer, anti-mitotic, anti-inflammatory agents and cause tyrosinase inhibition, and nitric oxide inhibition.[14–16] In addition, chalcone is a starting material for the synthesis of several biologically active heterocycles such as benzothiazepines, pyrazolines, and flavones.[17] Therefore, this family has been utilized by researchers to design new derivatives or to obtain improvement of the yields of these products. Attempts are being made in order to find new pathways for synthesizing these compounds in easier and faster ways.

The Claisen–Schmidt condensation reaction is the best method for synthesizing chalcone derivatives by using strong bases such as sodium and potassium hydroxide, or acids such as dry HCl, and aluminumchloride.[18] Some of the organometallic catalysts such as Zn(bpy)(OAc)^{2},[19] have also been reported as catalysts for this reaction.

Moreover, chalcone can be synthesized by using the Suzuki reaction.[20] Although there are several pathways to prepare the chalcones, various disadvantages have been reported for these methods such as long reaction times (14 h to 5 days), high temperature, expensive catalysts and reagents, production of poisonous substances, use of hazardous solvents, production of several by-products and the neutralization process. Therefore, several studies were carried out to replace the conventional and commercial catalysts with heterogeneous materials. These catalysts led to reactions with mild conditions and more advantages such as saving time and energy and environmental friendliness. Mesoporous silica nanomaterials such as MCM-41 and SBA-15 have been introduced as suitable catalysts for the Claisen–Schmidt condensation reaction,[21,22] which can be carried out with or without presence of the solvent. Recently, the Claisen–Schmidt reactions carried out under solvent-free conditions by using mesoporous silica materials were reported as a green chemistry alternative in order to reduce the environmental pollution and bring down the handling costs due to the simplification of the work up technique.[21]

In a recent study, Romanelli *et al.*[22] synthesized aminopropylated nanosilica by a sol–gel process using tetraethyl orthosilicate (TEOS) as a source of Si, followed by functionalization with different amounts of 3-aminopropyltriethoxysilane (APTES) under toluene reflux. These modified nanoparticles catalyzed the synthesis of chalcones through the Claisen–Schmidt reaction under solvent-free conditions with high selectivity. These results show that the activity of the catalyst was increased over amino modified silica. Wang *et al.*[23] studied the Claisen–Schmidt condensation between benzaldehyde and acetophenone, and subsequently, intramolecular over the aminopropyl-functionalized SBA-15 with well-ordered hexagonal structure. This catalyst was synthesized by the one-pot condensation of TEOS and APTES using amphiphilic block copolymer as the template under acidic conditions. The results exhibited a good activity and high selectivity for chalcone synthesis over this catalyst in the solvent-free conditions, while the use of organic solvents decreased the catalytic activity and selectivity.

In the present study, we synthesized protonated aluminate mesoporous silica nanoparticles (HAlMSN) as a solid acid catalyst and used it in order to improve the conditions of the Claisen–Schmidt condensation reaction. (*E*)-Chalcone derivatives as a biologically active family were selected due to their importance in the pharmaceutical science. Initially, MSN was prepared through the sol–gel process, then, HAlMSN solid catalyst was prepared through aluminum loading on MSN by the post-synthesis method followed by protonation. FTIR spectroscopy of adsorbed pyridine was used to investigate the acid strength of this catalyst. Physical properties of the samples were determined by nitrogen physisorption, XRD, FTIR and ^{27}Al solid state NMR. The mechanism of (*E*)-chalcone synthesis in the Claisen–Schmidt condensation over the HAlMSN solid acid catalyst under solvent-free conditions was studied in detail. The advantages of using the HAlMSN catalyst, such as high activity, short time and low temperature in this reaction, were studied in detail and a comparison of its activity with the commercial and the different heterogeneous catalysts was carried out.

Experimental

Catalyst synthesis

The synthesis of pure MSN followed the procedure of the previous report[3] and is described below. Cetyltrimethylammonium bromide (CTAB, 1.17 g) was dissolved in a solution containing double distilled water (180 g) and 1,2-propanediol (30 mL) in an aqueous ammonia solution (7.2 mL, 25%). After vigorous stirring for approximately 30 min at 323 K, tetraethylorthosilicate (TEOS, 1.43 mL) and 3-aminopropyl triethoxysilane (APTES, 0.263 mL) were added to the mixture. The resulting mixture was stirred for an additional 2 h at 323 K and allowed to rest for 20 h at the same temperature. The gel composition used in the synthesis of MSN was 1 TEOS : 0.17 APTES : 0.5 CTAB : 13.5 NH_3 : 85.2 PD : 1042 H_2O. The sample was collected by centrifugation at 20 000 rpm for 30 min and washed with deionized water and absolute ethanol three times. The surfactant was removed by heating MSN (1 g) in an NH_4NO_3 (0.3 g) and ethanol (40 mL) solution at 333 K. The surfactant-free product was collected by centrifugation and dried at 383 K overnight prior to calcination in air at 823 K for 3 h. The acidic sites of the sample were prepared by aluminum-grafting (calculated Si/Al = 20) on the template-free MSN at 353 K for 10 h, followed by centrifugation and drying at 383 K overnight, prior to calcination in air at 823 K for 3 h. Sodium aluminate (Sigma-Adrich) was used as a precursor of aluminum. The aluminum-grafted MSN was denoted AlMSN. Whereas, the protonated AlMSN (HAlMSN) was prepared by protonation of AlMSN (1 g) using an aqueous solution of NH_4NO_3 (2.5 g in 50 mL of double distilled water) at 333 K for 16 h, followed by removal of solution, drying at 383 K overnight and calcination at 823 K for 3 h in air.

Catalyst characterization

The crystallinity of the catalysts was measured with a Bruker Advance D8 X-ray powder diffractometer with Cu Kα ($\lambda = 1.5418$

Å) radiation as the diffracted monochromatic beam at 40 kV and 40 mA. Nitrogen physisorption analysis was conducted on a Quantachrome Autosorb-1 at 77 K. Before the measurement, the sample was evacuated at 573 K for 3 h. Elemental analysis of the catalyst was carried out with an Agilent 4100 Microwave Plasma-Atomic Emission Spectrometer. ^{27}Al MAS NMR spectra were recorded on a Bruker Avance 400 MHz spectrometer at 104.3 MHz with 0.3 s recycle delays, and spun at 7 kHz to determine the chemical status of aluminum in the silicate framework of the catalysts.

Fourier Transform Infra-Red (FTIR) measurements were carried out using an Agilent Cary 640 FTIR Spectrometer. The catalyst was prepared as a self-supported wafer and activated under H_2 stream ($F_{H_2} = 100$ mL min^{-1}) at 623 K for 3 h, followed by vacuum conditions at 623 K for 1 h.[24] To determine the catalyst acidity, the activated samples were exposed to 2 Torr of pyridine at 423 K for 30 min, followed by evacuation at 473 K for 1 h to remove the physisorbed pyridine. All spectra were recorded at room temperature. In order to compare the surface coverage of the adsorbed species between different wafer thicknesses, all spectra were normalized using the overtone and combination vibrations of the MSN lattice between 2200 and 1300 cm^{-1} after activation, particularly the lattice peaks at 1855 cm^{-1}.[25]

The bulk Si/Al ratio of HAlMSN was determined by using a Bruker S4 Explorer X-ray Fluorescence (XRF) Spectrometer, using Rh as the anode target material, operated at 20 mA and 50 kV. The analysis showed that the Si/Al ratio of the HAlMSN framework was 18.9.

The concentration of pyridine adsorbed on Brønsted and Lewis acid sites was determined based on the report of Emeis.[26] The number of Brønsted and Lewis acid sites was calculated using the integrated molar adsorption coefficient values. The resulting values were $\varepsilon_{1545} = 1.67$ cm μmol^{-1} for the band at 1545 cm^{-1}, which is characteristic of pyridine on Brønsted acid sites and $\varepsilon_{1455} = 2.22$ cm μmol^{-1} for the 1455 cm^{-1} band of pyridine on Lewis acid sites.

Catalytic activity

The catalytic activity of the HAlMSN catalyst was investigated using the Claisen–Schmidt condensation reaction. The details of this study are explained in the following section.

Typical experimental protocol

To a stirring mixture of aldehyde (0.02 mol), ketone (0.04 mol) and dichloromethane (0.15 mol), HAlMSN (0.01 wt%) was added at room temperature and the stirring was continued for 30 min. The mixture was heated at 323 K under an air atmosphere for 3 h (Table 2). The samples were taken at regular intervals and the concentrations of ketones (acetophenone derivatives) and chalcones were identified by GC-Mass spectrometry (detector HP 5971) and analysed using chrompak CP 9000 GC equipped with an RTX-50 capillary column and a flame ionization detector. The dodecane was chosen for the internal standard.

The conversion of ketone to chalcone ($X_{chalcone}$%), the yield of chalcone ($Y_{chalcone}$%) and the selectivity of chalcone ($S_{chalcone}$%) were calculated according to eqn (1)–(3), respectively:

$$X_{chalcone}(\%) = \frac{[KET]_i - [KET]_f}{[KET]_f} \times 100 \quad (1)$$

$$Y_{chalcone}(\%) = \frac{n_y}{n_c} \times 100 \quad (2)$$

$$S_{chalcone}(\%) = \frac{n_y}{n_i - n_f} \times 100 \quad (3)$$

where $[KET]_i$ and $[KET]_f$ are the concentrations of ketone at the initial and final reaction times, respectively; n_y and n_c are the number of moles of the yielded and calculated (*E*)-chalcones, respectively; and n_i and n_f are the number of moles of ketone at the initial and final reaction times, respectively.

Reusability testing

The reusability of the HAlMSN catalyst for the (*E*)-chalcone production (%) at 298 K was tested after it was used five times.[27] The catalyst was washed with hot toluene (3 × 10 mL) and dried under vacuum at 343 K for 4 h. The weight of the catalyst, its catalytic activity and the product were measured after each reaction. After reusability testing, the catalyst was subjected to XRD and FTIR in order to study its properties.

Results and discussion

Catalyst characterization

Fig. 1 shows the XRD patterns of MSN and HAlMSN. These catalysts have presented three peaks at 2.30°, 4.20° and 4.70°, corresponding to 100, 110 and 200, respectively. The sharp peaks at 2.30° reveal the high order crystalline structures of the catalysts and confirm the two-dimensional hexagonal (*p6mm*) structure with d_{100}-spacing of approximately 3.8 nm and an average lattice constant (a_0) of 4.4 nm (Table 1).

In addition, this peak illustrates the long ordered structure in MSN.[28] The intense peak at 2.30° decreased in HAlMSN and

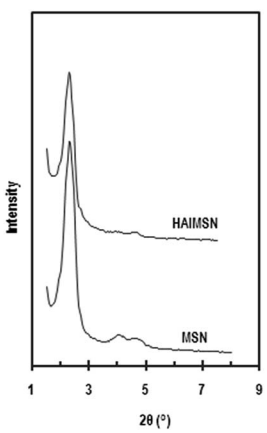

Fig. 1 XRD patterns of MSN and HAlMSN.

Table 1 Physical properties of MSN and HAlMSN[a]

Sample	d_{100} (nm)	a_0 (nm)	S (m^2 g^{-1})	V_p (cm^3 g^{-1})	W (nm)	t (nm)
MSN	3.84	4.43	995	0.84	3.38	1.06
HAlMSN	3.76	4.34	639	0.54	3.38	0.96

[a] d_{100}, d-value of reflection 100; a_0, pore center distance is equal to $d_{100} \times 2/\sqrt{3}$; S, BET surface area (m^2 g^{-1}) obtained from N_2 adsorption; V_p, total pore volume (mL g^{-1}); W, pore size (nm) obtained from the BJH method; t, pore-wall thickness is equal to $a_0 - W$.

Table 2 Synthesis of (*E*)-chalcones (**3a–h**) using the HAlMSN solid acid catalyst[a]

Entry	R	R′	Time (h)	Conv. (%)	Select. *E*-isomer (%)	Yield (%)	Ref.
1[a]	H	H	3	97	94	91	38
2[b]	H	4-Cl	3	94	87	82	24
3[c]	H	2-OH	3	96	90	86.5	24
4[d]	4-OMe	4-OMe	3	96	95	91	37
5[e]	4-OH	4-OCH_3	3	98	94	92	37
6[f]	H	4-OCH_3	3	97	91	88	24
7[i]	4-OMe	H	3	98	90	88	39
8[k]	H	2,6-Cl	3	97	88	85.4	37
9[g]	4-OH	H	3	96	91	87.4	39
10[h]	4-Me	3-Cl	3	95	92	87.4	37

[a] a–h are the various (*E*)-chalcones with the various substitutions of R and R′.

shifted to 2.25°, which indicated the loading of Al into the HAlMSN framework and led to an increase in the interplanar spacing of MSN. This shifting of the intense peak is probably due to the presence of a residual sodium atom that interacted with the Si atom through the O atom.[7] A decrease in the intensity of the peak in HAlMSN indicates a less uniform crystal structure compared to MSN.

Table 1 shows the physical characteristics of the MSN and HAlMSN catalysts. The surface areas of MSN and HAlMSN are 995 and 639 m^2 g^{-1}, respectively. The change in the BET specific surface area is probably due to the alteration in the pore size distributions and the change in the two dimensional hexagonal structure of MSN. The grafting of MSN with sodium aluminate has plugged MSN at a pore diameter of around 2–5 nm (Fig. 2).

However, the protonation of AlMSN removed this plugging from MSN, therefore, their pore sizes remained in a constant value. This result is also in good agreement with the alteration of total pore volume and pore-wall thickness of MSN obtained from the BJH method analysis (Table 1).

The plugging of MSN decreased the total pore volume from 0.84 to 0.54 cm^3 g^{-1}, whereas, the pore-wall thickness shrank from 1.06 to 0.96 nm due to the widening of the pore size of MSN. These revealed that Al and residual Na were located inside and outside of the pores in HAlMSN. Decreases in the d_{100}-spacing value and unit cell parameter indicate the immobilization of Al in the framework and the changing of the HAlMSN structure.[29]

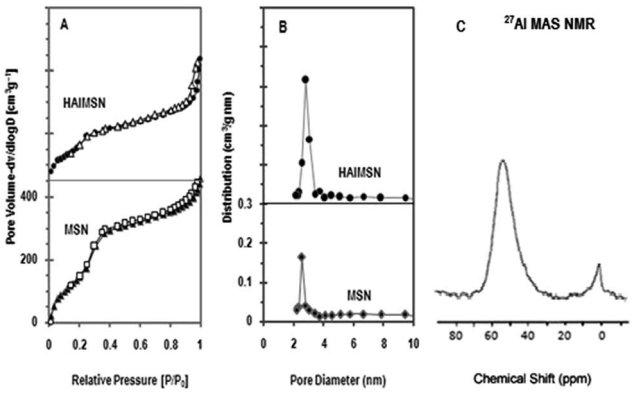

Fig. 2 (A) Nitrogen sorption isotherm and (B) pore size distributions for MSN and HAlMSN; (C) ^{27}Al MAS NMR spectrum of HAlMSN.

Fig. 2 shows the nitrogen sorption isotherms and the pore size distribution of MSN and HAlMSN. Fig. 2A shows that the isotherm representing MSN can be classified as type IV with a type H4 hysteresis loop, which can be attributed to the mesoporous structures. The MSN isotherm illustrates the properties of an intense inflection of the capillary condensation within uniform pores at $P/P_0 = 0.2$–0.4, which indicates the presence of MSN of small pore diameter and volume.[30] At $P/P_0 = 0.8$–1.0 the increase in adsorbed nitrogen illustrates an important external surface area contribution. At relative pressure of P/P_0 less than 0.2, gradual and rounded transitions showed the presence of a small number of non-slit-like micropores, whereas the pore size distribution confirmed the presence of a narrow peak at a pore diameter of 2.5–2.8 nm, Fig. 2B. In HAlMSN, the inflection of the isotherm at $P/P_0 = 0.8$–1.0 increased gradually, indicating the presence of extra-framework Al that contributed to the external surface area, and the inflection at $P/P_0 < 0.2$ decreased due to the presence of Al species inside the microporous MSN.

In agreement with our results, On *et al.* immobilized Al into an MCM-41 mesoporous framework with the Si/Al of 33.[31] The X-ray diffraction result showed that the ordered hexagonal structure of the parent MCM-41 did not change and exhibited a d-spacing of *ca.* 40 and 41 Å for MCM-41 and Al-MCM-41, respectively. Both samples represented the narrow pore size distributions of around 28 Å with the surface areas of 1050 and 815 m^2 g^{-1} for MCM-41 and Al-MCM41, respectively.

Fig. 2C shows the peaks of the ^{27}Al MAS NMR spectrum of the HAlMSN solid catalyst. Here, no peak was observed for MSN, while the peaks at approximately 53 and 0 ppm were observed for HAlMSN, which are responsible for the octahedral and tetrahedral Al atoms, respectively.[32] The peaks of the 6-coordinate structure (extra-framework) illustrate that a small part of the aluminum was dislodged into the aluminosilicate framework.[33,34] Most of the Al species remained in the 4-coordinate structure (framework), which is promising for the catalytic reactions. Chen *et al.* reported the synthesis of Al-MCM-41 by the loading method, in the various Si/Al ratios and showed two types of Al structure in the MCM-41 frameworks.[33]

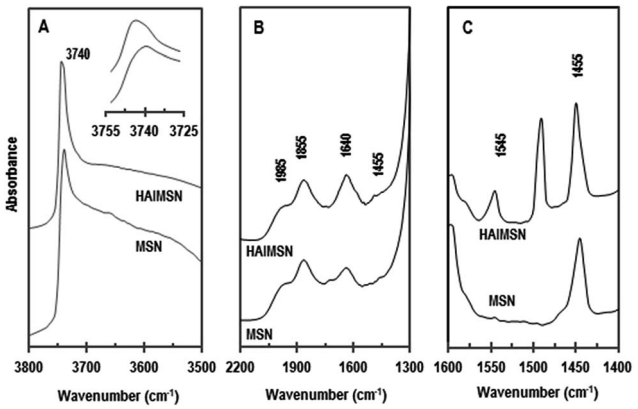

Fig. 3 FTIR spectra of MSN and HAlMSN (A) in the region of 3800–3500 cm^{-1}, (B) in the region of 2200–1300 cm^{-1}, (C) pyridine adsorbed FTIR.

The FTIR and pyridine adsorbed FTIR spectra of MSN and HAlMSN are shown in Fig. 3. The pure MSN catalyst did not show the Brønsted acid sites due to its electrically neutral properties. The non-acidic silanol groups of MSN observed in the range of 3800–3500 cm^{-1} are shown in Fig. 3A. The sharp band at 3740 cm^{-1} is attributed to the non-acidic terminal silanol groups (≡SiOH) placed on the external surface of MSN.[35]

Introduction of Al into the mesoporous silica decreased H-bonds of the terminal hydroxyl groups, and the structural defects. The intense band at 3740 cm^{-1} shifted to 3745 cm^{-1} after protonation, indicating the production of geminal silanol groups due to the dislodging of Al from the framework.[12] There are no significant differences in the band intensities in the region of 3740 cm^{-1} for MSN and HAlMSN, which illustrates that they have a comparable primary particle size and have no significant differences in the d_{100}-spacing or pore diameters. Fig. 3B shows the vibrational lattice stretching frequency of the mesoporous silica catalysts in the region of 2200–1300 cm^{-1}. The bands observed at 1855 and 1640 cm^{-1} probably correspond to Si–O–Si bonds. Aluminum loading and protonation intensified the band at 1640 cm^{-1}, which may correspond to an increase in the concentration of Si atoms connected to Al or H atoms through O atoms.

The number and strength of the catalyst acid sites was evaluated using pyridine adsorptions monitored by IR spectroscopy. IR spectra of the adsorbed pyridine on MSN and HAlMSN in the region of 1600–1400 cm^{-1} are shown in Fig. 3C. The presence of absorbance bands at 1455 and 1545 cm^{-1} are indicative of the Lewis and Brønsted acid sites, respectively, while the absorbance band at around 1495 cm^{-1} is attributed to the combination of the Lewis and Brønsted acid sites.[35,36]

The pure MSN possesses only Lewis acid sites at 1455 cm^{-1}, which belong to the electron pair acceptor sites of silanol groups. Incorporation of Al increased Lewis acidity and protonation of Al-grafted MSN generated strong Brønsted acid sites at 1545 cm^{-1}, which probably correspond to the formation of acidic hydroxyl groups (OH groups that bind Si or Al in the framework) and/or bridging hydroxyl (Si(OH)Al) groups.[36,37]

The concentrations of Brønsted and Lewis acid sites for HAlMSN were calculated to be 96 μmol g^{-1} for the Brønsted sites and 189 μmol g^{-1} for Lewis acid sites.[3]

These values were measured in terms of amounts of the pyridine ion for the Brønsted sites with corresponding band at 1545 cm^{-1}, and for Lewis acid sites with corresponding band at 1455 cm^{-1}.[26]

The morphology of the HAlMSN was observed using FESEM and TEM images. Fig. 4 shows the HAlMSN as a uniform spherical particle with particle size of 70–120 nm. The 2D hexagonal mesostructure was confirmed by TEM images. These images clearly show well-ordered pores with parallel and cylindrical channels and honeycomb structures, which indicate a 2D hexagonal *p6mm* mesostructure for HAlMSN.[38] These results are in accordance with those measured from the low-angle XRD patterns and N_2 sorption analysis.

Catalytic activity

Chalcones are usually synthesized by using the Claisen–Schmidt condensation reaction under basic or acidic conditions in the presence of a polar solvent. This reaction involves a difficult purification process as the condensation reaction often leads to a complex mixture.[39,40] HAlMSN catalysed the (*E*)-chalcones (**3a–h**) synthesis, which was carried out with acetophenone (**1**) and benzaldehydes derivatives (**2**) under solvent-free conditions at low temperatures, with excellent yield and selectivity, without the generation of any side product and in a short time (Scheme 1). In these reactions the (*Z*) isomers were synthesized as by-products in small amounts. These one-pot reactions occurred by focusing on the optimization of the reaction conditions in terms of the amounts of products, temperature and reaction time.

To compare the results of the reaction in the presence and absence of the catalyst, the reaction was also carried out through the traditional method without catalyst, at 323 K. No improvement in the reaction yield was observed. The use of

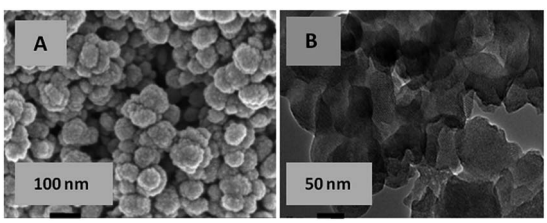

Fig. 4 FESEM (A) and TEM (B) images of HAlMSN.

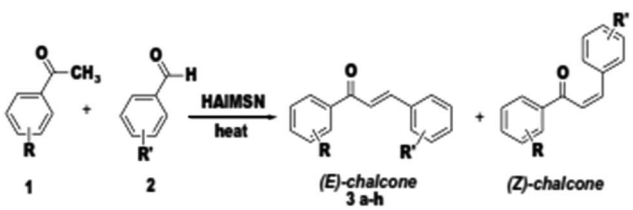

Scheme 1 Reagents and conditions for the synthesis of (*E*)-chalcones.

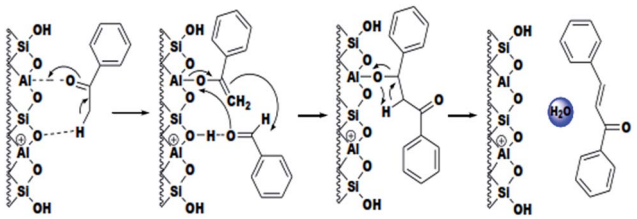

Scheme 2 Proposed mechanism of the (*E*)-chalcone synthesis over HAlMSN.

high polarity solvents such as light alcohols gave a small yield, which was probably due to the solvent effect.[23]

The HAlMSN solid acid catalyzed the synthesis of (*E*)-chalcone derivatives. The selective production of (*E*)-1,3-diphenyl-2-propenone derivatives was smooth and high yields were obtained. The proposed mechanism described the formation of an enolate intermediate through the bond formation between carbonyl groups and oxygen atoms of Al–O bands in HAlMSN (Scheme 2).

This mechanism suggests that the bond formation occurs by the reaction of Al^{3+} ion species with the oxygen of the aryl ketone carbonyl group, in order to generate the enolate intermediate by the abstraction of a proton from the α-carbon of the aryl ketone. The reaction proceeds through the further coordination with the aryl aldehyde, increasing the electrophilicity of the aldehyde carbonyl group, thus making it susceptible to intramolecular nucleophilic attack by the enolate ion. A further dehydration process leads to the resultant products (**3a–h**). The catalyst was recovered and can be recycled five times without appreciable loss of reactivity.

Reuse of the catalyst

In order to investigate the reusable properties of the HAlMSN catalyst, a recycling experiment was conducted and the result is shown in Fig. 5. After reaction, the catalyst was recycled by washing with hot toluene (3 × 10 mL) and drying under vacuum at 343 K for 4 h. The catalyst was reused five times without a serious loss in the catalyst weight, catalytic activity and product selectivity during each recycling process.

A decrease in the conversion of the substrate to (*E*)-chalcone was not noticeable (there was a reduction from 97 to 94%), which indicates the good reusability of this catalyst under these reaction conditions.[41]

The XRD results (not shown) of HAlMSN before and after the Claisen–Schmidt reactions indicate that there was no significant change after the reaction. However, the presence of two weak bands observed at 2860 and 2930 cm^{-1} in the IR spectra, correspond to the C–H stretching vibrations, which may be related to the plugging of the unreacted acetophenone and/or chalcone molecules remaining on the pores. Removal of the plug by washing with toluene reduced these two bands at 2860 and 2930 cm^{-1} to the initial values. Fig. 6 shows the FTIR spectra of the fresh HAlMSN, after the Claisen–Schmidt reaction at 473 K for 3 h and after washing with toluene at the end of the final step.

Table 3 shows the comparison study of the (*E*)-chalcone synthesis over several types of heterogeneous catalysts.[41–45] The results indicate higher activity of HAlMSN in (*E*)-chalcone synthesis, in comparison with the other catalysts such as traditional catalysts, pure MSN, ZSM-5, SBA-15, MCM-41 and MgO. This is probably due to the presence of stronger Lewis and Brønsted acid sites in HAlMSN. The larger pore size and surface area of this catalyst also provide enough space for reaction of the reactants with the active sites inside the catalyst wall. The results in Table 3 show that HAlMSN exhibits more activity in comparison with the mentioned catalysts, based on shorter reaction time (3 h), lower temperature and higher yield of (*E*)-chalcone.

In Fig. 7A the conversion of the reaction with the different substitutes (**3**) *versus* reaction time are presented. The results show that for the (*E*)-chalcones with electron donating

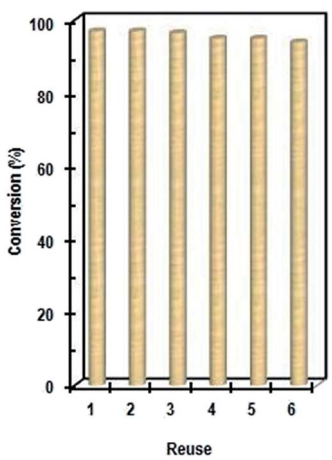

Fig. 5 Stability of HAlMSN in the Claisen–Schmidt reaction at 298 K, after it was reused five times.

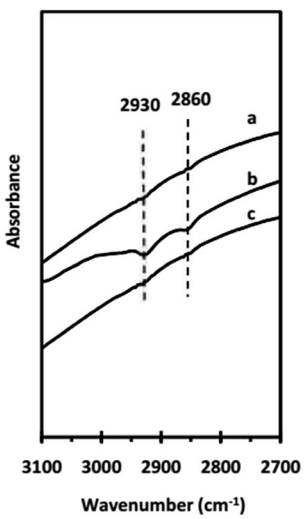

Fig. 6 FTIR spectra of (a) fresh, (b) used and (c) washed HAlMSN in the C–H stretching regions. Chalcone production was done at 473 K for 3 h.

Table 3 Comparison of (*E*)-chalcone yield over HAlMSN and the other homogeneous and heterogeneous catalysts

Catalyst	Conv. (%)	Yield (%)	Select.[a] (%)	Time (h)	Temp. (K)	Ref.
Blank	13.1	12.9	98.5	6	423	43
H_2SO_4	98	71.2	72.7	6	423	41
$NaHCO_3$	—	62.2	—	24	393	44
HAlMSN	97	92	95	3	298	This study
MSN	10.5	7.2	68.2	6	423	This study
SiO_2(230–280 mesh)	6	2.6	—	6	413	45
Zn–Al(6)	66.4	34.1	—	6	413	45
SBA-15	9.7	6.2	63.9	6	423	41
ZSM-5	17.7	10.9	61.6	6	423	41
MCM-49	13.7	13.7	100	6	423	41
SBA-15-SO_3H	50	41.7	83.4	6	423	41
Al(11)SBA-15-SO_3H	88.7	87.3	98.4	6	423	41
MgO	40	—	—	18	523	42

[a] The selectivity of (*E*)-chalcone.

substituents, there is higher conversion in the Claisen–Schmidt reaction in comparison to those with electron withdrawing substituents. The reaction time with electron donating substituents is less than that with electron withdrawing substituents. The lone pair electrons with enough activation energy react with the Lewis acid sites of HAlMSN and consequently, the conversion of starting material to the product occurs with higher yield and selectivity.

Fig. 7B shows the number of moles of (*E*)-chalcone and starting materials that were produced or consumed during the Claisen–Schmidt reaction. Here, the consumption of starting materials and production of (*E*)-chalcone was investigated. The number of moles of benzaldehyde and acetophenone were reduced while the number of moles of (*E*)-chalcone increased. In this reaction, acetophenone is the limiting reagent and as was expected, the acetophenone was almost completely consumed, while benzaldehyde remained in the container. The results confirm that the amount of the product depends on the amount of acetophenone as the limiting reagent.

In the (*E*)-chalcone synthesis, the turnover frequency (TOF) is the number of moles of (*E*)-chalcone that a mole of HAlMSN can produce per unit time, before becoming inactive. Here, TOF was determined from the rate of (*E*)-chalcone synthesis and the number of Brønsted acid sites. The TOF of (*E*)-chalcone synthesis over HAlMSN is shown in Fig. 8. Although the TOF increased with the reaction time, it became constant after 180 minutes, which indicates that the highest yield of (*E*)-chalcone was obtained after 3 h.

The effect of the benzaldehyde to acetophenone (B/A) molar ratio

The influence of the benzaldehyde/acetophenone (B/A) molar ratio on the conversion of acetophenone to (*E*)-chalcone using HAlMSN is shown in Fig. 9. The effect of the B/A molar ratios of 1 : 1, 1 : 2, 2 : 1, 3 : 1 and 4 : 1 on the production of (*E*)-chalcone in Claisen–Schmidt condensation were studied. After the condensation reaction was carried out for 3 h, the (*E*)-chalcone yield decreased from 97% to 68% from the B/A ratio of 1 : 2 to 4 : 1, respectively.

This result is probably due to the presence of excess benzaldehyde surrounding the active sites, which could have a blocking-effect on improving the catalytic activity of the Claisen–Schmidt reaction. On the other hand, the excess benzaldehyde diluted the concentration of acetophenone in the media, consequently decreasing the contact probability between acetophenone molecules and the active acid sites on the surface of HAlMSN. The results show that the highest product of (*E*)-chalcone synthesis was observed with a 1 : 2 molar ratio of B/A.

The obtained results are in strong agreement with the results of Li *et al.*[27] They synthesized chalcone *via* a condensation reaction over the Al-SBA-15-SO_3H acid catalyst, under solvent-free

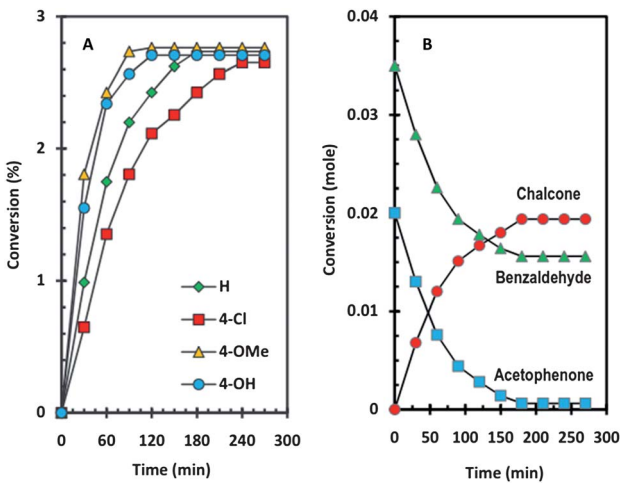

Fig. 7 (A) Development of the production of (*E*)-chalcone derivatives during the reaction time, (B) the moles of benzaldehyde, acetophenone and (*E*)-chalcone produced during the Claisen–Schmidt reaction process.

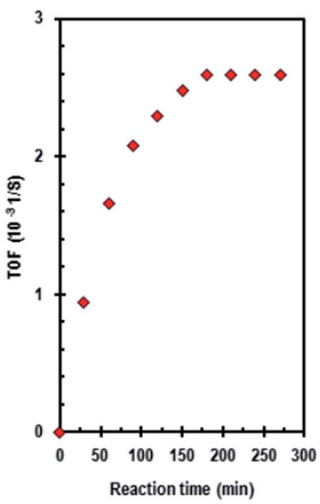

Fig. 8 Turnover frequency of (*E*)-chalcone production during the Claisen–Schmidt reaction.

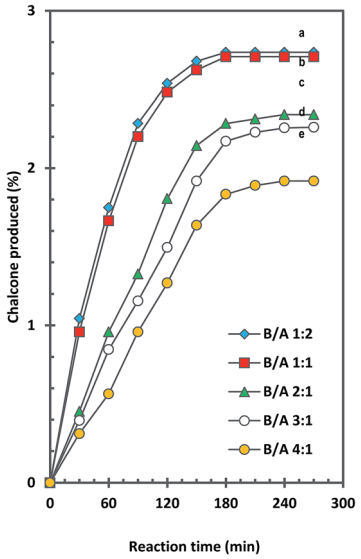

Fig. 9 The effects of the benzaldehyde/acetophenone (B/A) molar ratio on the conversion of acetophenone in (*E*)-chalcone synthesis.

conditions. They reported that the amount of acetophenone decreased from 89.0% to 72.1% by changing the molar ratio of B/A from 1 : 2 to 5 : 1, and the yield of synthesized chalcone decreased from 86.9% to 66.1%.

Conclusions

The HAlMSN solid acid catalyst was synthesized by using a post-synthesis method from MSN followed by protonation. X-ray diffraction and N_2 sorption results confirmed the ordered mesoporous structure with pore diameter of 3.38 nm, and surface areas of 995 and 639 $m^2\ g^{-1}$ for MSN and HAlMSN, respectively. ^{27}Al solid state NMR and IR results confirmed that Al grafting followed by protonation produced extra-framework aluminum atoms which led to the generation of strong Brønsted and Lewis acid sites, in which the pyridine probe molecules remained after outgassing at 473 K.

HAlMSN catalyzed the Claisen–Schmidt condensation reaction as a strong solid acid. The (*E*)-chalcone derivatives with biological activity were synthesized over this catalyst with excellent yield and selectivity. The outstanding advantages of this solid catalyst include high yield and selectivity, low temperature, fast work up and short reaction time. This catalyst is also compatible with both solvent and solvent-free conditions.

The conversion of ketone to chalcone was 97% at 298 K in the presence of the HAlMSN as a solid acid catalyst. HAlMSN was reused five times while maintaining the high yield production of (*E*)-chalcone, which indicates the high stability of this catalyst. The highest yield of (*E*)-chalcone synthesis was observed with a 1 : 2 molar ratio of B/A. The result of the Claisen–Schmidt reaction indicates that HAlMSN is able to catalyze the chemical reactions under mild conditions with high efficiency, reduced reaction time, low energy consumption and environmental friendliness.

Acknowledgements

This work was supported by the University Teknologi Malaysia under RUG Project No. 06H17 and special thanks to North Tehran Branch, Islamic Azad University for helping in this research.

References

1 M. A. A. Aziz, A. A. Jalil, S. Triwahyono, R. R. Mukti, Y. H. Taufiq-Yap and M. R. Sazegar, *Appl. Catal., B*, 2014, **147**, 359.
2 S. Shen, J. Chen, R. T. Koodali, Y. Hu, Q. Xiao, J. Zhou, X. Wang and L. Guo, *Appl. Catal., B*, 2014, **150–151**, 138.
3 M. R. Sazegar, A. A. Jalil, S. Triwahyono, R. R. Mukti, M. Aziz, M. A. A. Aziz, N. H. N. Kamarudin and H. D. Setiabudi, *Chem. Eng. J.*, 2014, **240**, 352.
4 N. H. N. Kamarudin, A. A. Jalil, S. Triwahyono, M. R. Sazegar, S. Hamdan, S. Baba and A. Ahmad, *RSC Adv.*, 2015, **5**, 30023.
5 S. Triwahyono, A. A. Jalil and M. Musthofa, *Appl. Catal., A*, 2010, **372**, 90.
6 S. Triwahyono, A. A. Jalil, R. R. Mukti, M. Musthofa, N. A. M. Razali and M. A. A. Aziz, *Appl. Catal., A*, 2011, **407**, 91.
7 H. D. Setiabudi, A. A. Jalil, S. Triwahyono, N. H. N. Kamarudin and R. R. Mukti, *Appl. Catal., A*, 2012, **417–418**, 190.
8 T. Kugita, S. K. J. T. Owada, N. Hashimoto, M. Onaka and S. Namba, *Appl. Catal., A*, 2003, **245**, 353.
9 J. Zhu, T. Wang, X. Xu, P. Xiao and J. Li, *Appl. Catal., B*, 2013, **130–131**, 197.
10 N. W. C. Jusoh, A. A. Jalil, S. Triwahyono, H. D. Setiabudi, N. Sapawe, A. H. Karim, N. H. N. Kamarudin, R. Jusoh, N. F. Jaafar, N. Salamun, M. A. H. Satar and J. Efendi, *Appl. Catal., A*, 2013, **468**, 276.
11 N. N. Ruslan, N. H. A. Fadzlillah, A. H. Karim, A. A. Jalil and S. Triwahyono, *Appl. Catal., A*, 2011, **406**, 102.
12 M. Liu, P. Wilairat and M. L. Go, *J. Med. Chem.*, 2001, **44**, 4443.
13 N. H. N. Kamarudin, A. A. Jalil, S. Triwahyono, V. Artika, N. F. M. Salleh, A. H. Karim, N. F. Jaafar, M. R. Sazegar, R. R. Mukti, B. H. Hameed and A. Johari, *J. Colloid Interface Sci.*, 2014, **421**, 6.
14 M. Satyanarayana, P. Tiwari, B. K. Tripathi, A. K. Srivastava and R. Pratap, *Bioorg. Med. Chem.*, 2004, **12**, 883.
15 J. Rojas, M. Paya, J. N. Dominguez and M. L. Ferrandiz, *Bioorg. Med. Chem. Lett.*, 2002, **12**, 1951.
16 R. Y. Prasad, L. A. Rao, L. Prasoona, K. Murali and R. P. Kumar, *Bioorg. Med. Chem. Lett.*, 2005, **15**, 5030.
17 F. Micheli, F. Degiorgis, A. Feriani, A. Paio, A. Pozzan, P. Zarantonello and P. J. Seneci, *J. Comb. Chem.*, 2001, **3**, 224.
18 N. O. Calloway and L. D. Green, *J. Am. Chem. Soc.*, 1937, **59**, 809.
19 K. Irie and K. Watanabe, *Bull. Chem. Soc. Jpn.*, 1980, **53**, 1366.
20 S. Eddarir, N. Cotelle, Y. Bakkoura and C. Rolandoa, *Tetrahedron Lett.*, 2003, **44**, 5359.
21 G. Nagendrappa, *Resonance*, 2002, **7**, 64.

22 G. Romanelli, G. Pasquale, A. Sathicq, H. Thomas, J. Autino and P. Vazquez, *J. Mol. Catal. A: Chem.*, 2011, **340**, 24.
23 X. Wang and S. Cheng, *Catal. Commun.*, 2006, **7**, 689.
24 A. Matsumoto, H. Chen, K. Tutsumi, M. Grun and K. Unger, *Microporous Mesoporous Mater.*, 1999, **32**, 55.
25 K. Kim, R. Ryoo, H. D. Jang and M. Choi, *J. Catal.*, 2012, **288**, 115.
26 C. A. Emeis, *J. Catal.*, 1993, **141**, 347.
27 W. Li, K. Xu, L. Xu, J. Hu, F. Ma and Y. Guo, *Appl. Surf. Sci.*, 2010, **256**, 3183.
28 S. Triwahyono, A. A. Jalil, N. N. Ruslan, H. D. Setiabudi and N. H. N. Kamarudin, *J. Catal.*, 2013, **303**, 50.
29 R. Mokaya, W. Jones, Z. Luan, M. D. Alba and J. Klinowski, *Catal. Lett.*, 1996, **37**, 113.
30 E. P. Ng, H. Nur, K. L. Wong, M. N. M. Muhid and H. Hamdan, *Appl. Catal., A*, 2007, **323**, 58.
31 D. Trong On, S. M. J. Zaidi and S. Kaliaguine, *Microporous Mesoporous Mater.*, 1998, **22**, 211.
32 L. Y. Chen, Z. Ping, G. K. Chuah, S. Jaenicke and G. Simon, *Microporous Mesoporous Mater.*, 1999, **27**, 231.
33 W. Hu, Q. Luo, Y. Su, L. Chen, Y. Yue, C. Ye and F. Deng, *Microporous Mesoporous Mater.*, 2006, **92**, 22.
34 M. Bevilacqua, T. Montanari, E. Finocchio and G. Busca, *Catal. Today*, 2006, **116**, 132.
35 J. A. Lercher and A. Jentys, in. *Introduction to Zeolite Science and Practice*, ed. J. Cejka, H. van Bekkum, A. Corma and F. Schuth, Elsevier, Amsterdam, 3rd revised edn, 2007, p. 452.
36 C. Morterra, G. Cerrato and G. Meligrana, *Langmuir*, 2001, **17**, 7053.
37 S. Li, A. Zheng, Y. Su, H. Zhang, L. Chen, J. Yang, C. Ye and F. Deng, *J. Am. Chem. Soc.*, 2007, **129**, 11161.
38 D. Trong On, S. M. J. Zaidi and S. Kaliaguine, *Microporous Mesoporous Mater.*, 1998, **22**, 211.
39 Y. Jeanvoine, J. G. Angyan, G. Kresse and J. Hafner, *J. Phys. Chem. B*, 1998, **102**, 5573.
40 D. G. Powers, D. S. Casebier, D. Fokas, W. J. Ryan, J. R. Troth and D. L. Coffen, *Tetrahedron*, 1998, **54**, 4085.
41 A. Sinhamahapatra, N. Sutradhar, B. Roy, P. Pal, H. C. Bajaj and A. B. Panda, *Appl. Catal., B*, 2011, **103**, 378.
42 B. M. Choudary, K. V. S. Ranganath, J. Yadav and M. L. Kantam, *Tetrahedron Lett.*, 2005, **46**, 1369.
43 J. Yang, Q. Yang, G. Wang, Z. Feng and J. Liu, *J. Mol. Catal. A: Chem.*, 2006, **256**, 122.
44 Q. Xu, Z. Yang, D. Yin and F. Zhang, *Catal. Commun.*, 2008, **9**, 1579.
45 L. B. Kunde, S. M. Gade, V. S. Kalyani and S. P. Gupte, *Catal. Commun.*, 2009, **10**, 1881.